

## NUMERICAL STUDY ON AEROTHERMAL PERFORMANCE OF SHROUD MOVEMENT IN THE VICINITY OF TURBINE TIPS

by

**Yunsong ZHANG<sup>a</sup>, Yongbao LIU<sup>a,b</sup>, Yujie LI<sup>a,b\*</sup>, and Qijie LI<sup>a</sup>**

<sup>a</sup> College of Power Engineering, Naval University of Engineering, Wuhan, China

<sup>b</sup> Military Key Laboratory for Naval Ship Power Engineering,  
Naval University of Engineering, Wuhan, China

Original scientific paper

<https://doi.org/10.2298/TSCI200628321Z>

*In this paper, the effects of shroud movement on transonic flow and heat transfer in the vicinity of turbine tip was studied by using 3-D simulation of GE-E<sup>3</sup> first-stage high pressure turbine. Aerothermal performance and flow structure were analyzed with and without turbine shroud moving, respectively. Based on the distribution of limiting streamlines and the vortex structures, the influential characteristics between the leakage flow and the secondary flow generated by shroud movement were studied. Moreover, the coefficient of heat transfer at the wall was investigated. Results show that the flow structure is changing with the movement of turbine shroud, and the location of the separation-line changes significantly by the influence of the secondary flow. The leakage vortex initial location delayed in axial direction and its breakdown point located at 65% cross-section. This accelerates the mixing loss and increase the perturbation. In addition, it is observed that the coefficient of average heat transfer is increased obviously by 54.8% in the region of shroud surface. However, this coefficient in the region of suction surface decreased by 11.9%.*

Key words: blade tip region, transonic flow, shroud movement, leakage vortex

### Introduction

To improve the performance of gas turbine, one typical way is to increase inlet temperature of high pressure turbine (HPT). However, the consequential design requirement increased due to the extreme working condition. In addition, the induced leakage flow mix with the main flow on suction surface, this phenomenon will decrease the working efficiency and increase the heat load in the vicinity of blade tips [1]. How to improve the working performance in the turbine blade tip region is becoming a hot research topic, and a lot of efforts have been done to study the turbine blade tip region in the design of the advanced gas turbine.

Generally, the experiment of heat transfer in the turbine blade tip region is conducted under the stationary condition. Representative work by Dong *et al.* [2], which measure the distance between blade tip and shroud by changing the relative position of the guided vane and the blade in a static single-stage cascade. The coefficient of blade tip heat transfer in upstream region fluctuates obviously, and the amplitude is 25% of the average value. Furthermore, Dong *et al.* [3] analyzed the separation and re-attachment of the flow in the blade tip region. Interaction mechanism between the tip separation bubble and the gap leakage flow is studied. Results show

\* Corresponding author, e-mail: liyujie028@163.com

that heat transfer coefficient (HTC) near the tip has a 30-50% fluctuation of the average value. The mechanism of HTC is analyzed theoretically and analytically by Yu [4] and Vadivelu [5]

Mayle *et al.* [6] and Metzger *et al.* [7] used a motor-driven rectangular cross-section turntable to realize the relative movement of the shroud. In the test, heat transfer characteristics of the blade tip and the groove-shaped blade tip were investigated, respectively. Results show that the HTC in the turbine blade tip region will be hardly affected by the movement. Srinivasan *et al.* [8] investigated heat transfer characteristics of the blade tip region at different clearance heights and obtained the consistent conclusions as Metzger *et al.* [7].

The aforementioned experimental studies found that the shroud has a small effect on heat transfer in the blade tip region and tip leakage flow is mainly affected by the pressure difference between the pressure and suction-side of the blade. Besides experiments, numerical study of turbine is another popular trend. Yang *et al.* [9] investigated the moving effect of the shroud on the aerodynamic performance of the annular cascade through 3-D numerical simulation [10]. It is indicated that the movement of the shroud significantly affects the aerothermal performance of the blade tip. Thorpe *et al.* [11] measured the heat distribution of the shroud under a typical turbine operating condition. They found that the highest heat load occurred around the leading edge of the rotating blades. Zakaria *et al.* [12] studied the effect of relative shroud movement on thermal load near the blade tip and further analyzed the mechanism of the secondary flow on the shroud wall surface.

In modern gas turbine, the velocity of leakage flow near the turbine blade tip can reach transonic during the high speed rotating process. While in the aforementioned literature, the phenomenon study is limited to subsonic flow condition and the shroud moves at a low speed [13]. In this paper, numerical simulation of GE-E<sup>3</sup> first-stage at a high relatively high speed of moving shroud are used to investigate the effects of shroud movement on transonic flow aerothermal performance in the blade tip region. The main passage flow and leakage vortex are analyzed and interaction mechanism between the secondary flow on the wall and the leakage flow in the gap are discussed.

## Computational method and validation

### *Calculation model, boundary conditions, and grid*

In this study, finite space method is used to discretize the space and governing equations which closed with a low Reynolds number turbulence model. Discrete space is adopted in high precision format while the heat transfer calculation adopts the total energy model considering fluid viscosity.

The research model is obtained by GE-E<sup>3</sup> high pressure turbine first-stage blade profile by a factor of 3 [14]. Tip clearance gap height equal to 1.5% blade height. The inlet total temperature is 550 K, inlet total pressure is 243 kPa, outlet static pressure is 150 kPa. Turbulent intensity and turbulent size are 0.097 cm and 1.5 cm, respectively. The wall surface is smooth without slip, wall temperature is 390 K and the shroud velocity is 320 m/s. The inlet air-flow angle is 32.01°.

The specific value of total pressure to static pressure is 1.41, and the specific value of total temperature to wall temperature is 1.62, which is consistent with the real turbine environment [15]. The shroud moves linearly while the blade is stationary. The direction is along the positive direction of the *Y*-axis. It is worth noting that when the shroud movement speed is 320 m/s, it is equivalent to the blade tip relative linear velocity when the rotor speed is about 8280 rpm.

The Autogrid5 module in NUMECA are used to generate the structured hexahedral grid. The blade tip gap area uses an O-type grid, and the mainstream flow area uses an H-shaped grid. The boundary-layer is encrypted to ensure that the maximum  $y^+$  is less than 2. The computation mesh is shown in fig. 1.

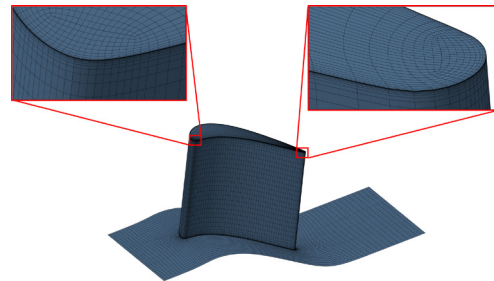


Figure 1. Computation mesh

To eliminate the effect of grids number on simulation calculation, three different sets of grids were selected to verify the irrelevance of the grids, including 1.37 million, 1.69 million, and 1.93 million grids, respectively. The number of nodes and the average HTC of blade tips of different grids are shown in tab. 1. Results show that the average HTC of blade tip will be little changed when the grids number is greater than 1.69 million. To get a better simulated aerothermal characteristics of blade tip, a denser grid is used in this paper (about 1.93 million).

Table 1. Grid independence

Mesh number	Average HTC	Relative error [%]
1.37 million	920.707	1.73
1.69 million	932.378	0.45
1.93 million	933.172	0.36
Extrapolation [16]	936.623	

### Turbulence model validations

The  $k-\omega$ , SST and SST  $\gamma-\theta$  turbulence models are comparatively analyzed with the experimental results of Kwak [17] and Azad [18]. The experimental operating parameters are shown in tab. 2. A tip clearance gap height of 1.97 mm (approximately equal to 1.5% blade height) was selected for the numerical simulation.

Table 2. Experimental operating parameters with Kwak [19] and Azad [20]

Case	Inlet total pressure	Inlet total temperature	Outlet static pressure	Turbulent intensity	Turbulent size	Wall temperature	Inlet flow angle
1	126.9 [kPa]	297 [K]	102.7 [kPa]	0.097	1.5 [cm]	340 [K]	32.01 [°]
2	143.0 [kPa]	297 [K]	108.3 [kPa]	0.097	1.5 [cm]	340 [K]	32.01 [°]

Figure 2 shows the comparison of predicted HTC on blade tip with the experimental data in Case 1. Generally, the simulation results of three turbulence models are basically consistent with the experimental result in the overall heat transfer distribution. The HTC on the pressure side of blade tip with SST model is slightly smaller than SST  $\gamma-\theta$  model. Results simulated by  $k-\omega$  model show that the overall value is higher and the high HTC region which the leading edge of blade suction side cannot be well simulated.

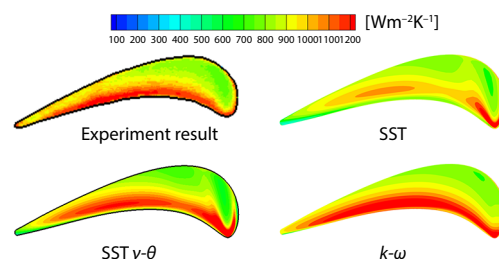


Figure 2. Comparison of predicted HTC on blade tip with the experimental data in Case 1

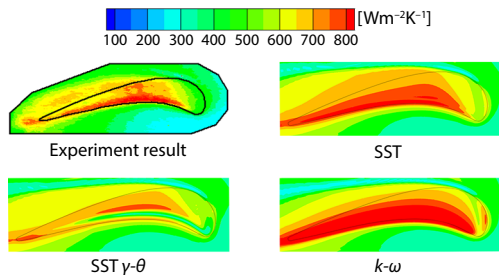


Figure 3. Comparison of predicted HTC on shroud with the experimental data in Case 1

Figure 4 shows the simulation results of the average HTC along the axial direction of blade tip with three turbulence models in Case 2. From 0-50% of the axial chord length, the simulated heat transfer values are higher than the experimental values. After that, the simulated values with SST  $\gamma$ - $\theta$  model and  $k$ - $\omega$  model are still higher than the experimental values, while the simulated results with SST model are lower than the experimental values. Therefore, SST with  $\gamma$ - $\theta$  model can better predict the HTC distribution on blade tip.

Figure 5 shows the results of the average HTC distribution on the suction surface from the 20% axial position the trailing edge. The values of  $k$ - $\omega$  model and SST model are higher than the experimental values. The axial position at 30-50% is lower than the experimental value, and in other positions are higher than the experimental value. In general, the SST  $\gamma$ - $\theta$  model is much closer to the experimental value.

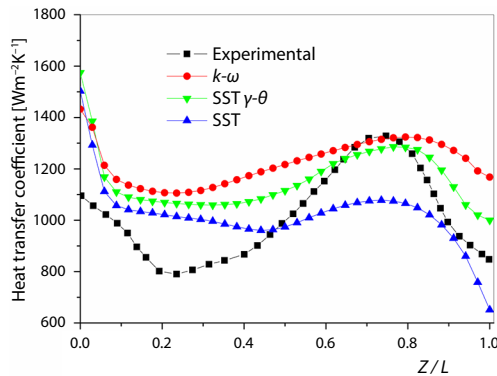


Figure 4. Comparison of predicted pitch wise-averaged HTC distribution along the axial direction with the experimental data in Case 2

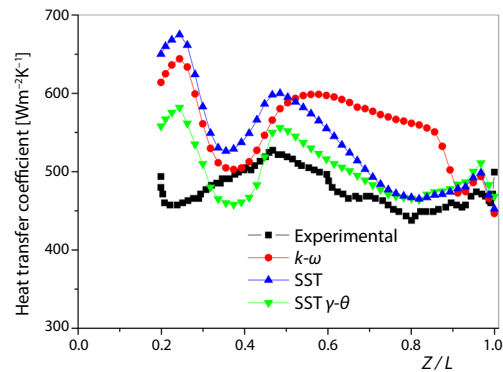


Figure 5. Comparison of predicted spanwise-averaged HTC distributions along the upper suction surface with the experimental data in Case 1

Based on the previous results, the SST  $\gamma$ - $\theta$  model has a better agreement with the experimental value. The heat transfer and transition in the tip region have higher accuracy, so the SST  $\gamma$ - $\theta$  model will be used for the simulation turbulence model in this paper.

## Results

### Flow and heat transfer characteristics

Figure 6 shows aerothermal characteristics and surface streamlines at the blade tip in the condition of shroud moving compared with stationary case. It includes the static pressure coefficient (SPC), isentropic Mach number, HTC and wall limit streamline.

The SPC is defined:

$$C_p = \frac{P - P_{in}^*}{0.5 \rho v_{in}^2} \quad (1)$$

where  $P$  stand for the local static pressure,  $P_{in}^*$  – the total pressure of the inlet,  $\rho$  – the gas density, and  $v_{in}$  – the speed of the inlet flow.

As can be seen from the SPC distribution, the high SPC is concentrated in the leading-edge area of blade tip, and the range of the high SPC expands when the shroud moves, mainly due to the flow stagnation and flow separation near the blade tip.

The isentropic Mach number distribution and the SPC distribution are basically the same. The shroud movement reduces the velocity of leakage flow on the pressure surface side compared to stationary shroud.

As can be seen from the HTC distribution, the high HTC area is mainly concentrated in blade leading edge. This can be obtained from the separation-lines (SL1, SL2) that after the leakage flow enters blade tip gap, leakage flow reattaches at the wall SL and generates a high HTC area. Since the movement of the shroud reduces the leakage flow velocity, SL2 is closer to the pressure surface than SL1, and the corresponding strip-shaped high heat transfer area is also closer to the pressure surface. When the case is stationary, a re-attachment line (RL1) is formed in the middle of the blade body, which is also the reason for the low HTC at the blue dotted line. From the aforementioned analysis, it can be found that the movement of the shroud has a greater impact on the flow and heat transfer characteristics of rotor blade.

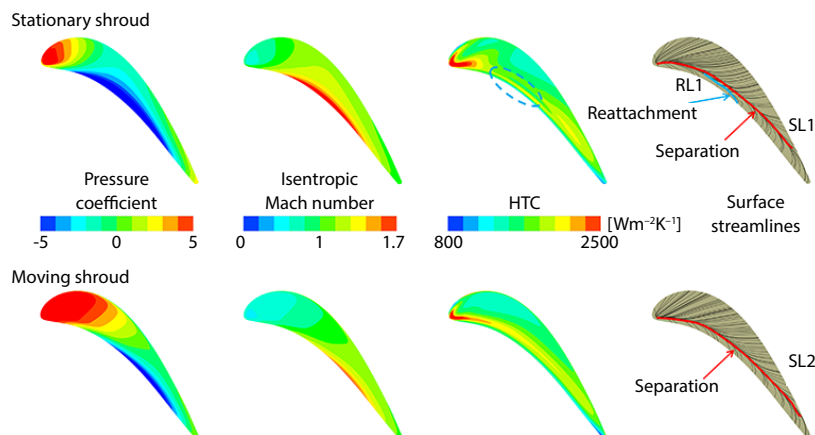


Figure 6. Aerothermal properties and surface streamlines at the tip

Figure 7 shows aerothermal properties and surface streamlines on the shroud wall. The distribution of the SPC and isentropic Mach number of the shroud area is basically consistent with the blade tip, but the HTC and the wall surface flow streamline distribution are significantly different.

From the result of the stationary case, there is no obvious high HTC area at the leading edge. The re-attachment line (RL2) formed by the leakage flow on the suction surface side and the main flow creates a long low HTC area. By the movement of the shroud, a large area of high HTC is formed on the pressure surface side. The main reason is that the deflection flow and leakage flow generated by the shroud movement has an impact on the shroud wall surface at the separation-line (SL3). Similarly, the leakage flow forms a re-attachment line (RL3) closer

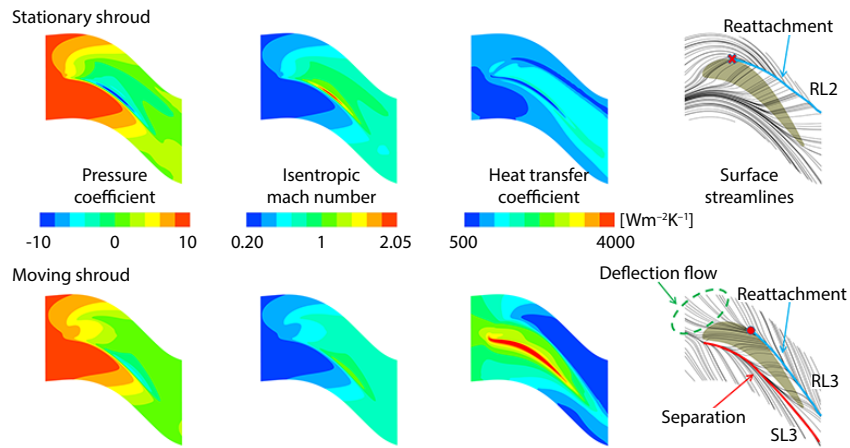


Figure 7. Aerothermal properties and surface streamlines on the shroud wall

to suction side. It is worth noting that the starting point of RL2 (the red cross point) is closer to leading edge than the starting point of RL3 (the red dot), in fig. 7.

Figure 8 shows the HTC distribution and wall surface flow streamline near the tip of the suction surface (from 15% axial position the trailing edge and 75% of blade height to the tip). In the HTC distribution, the white arrow indicates that high HTC area is formed by leakage vortex flow at suction surface. The high HTC area is horizontal with stationary case while the high HTC area is inclined when in the moving case.

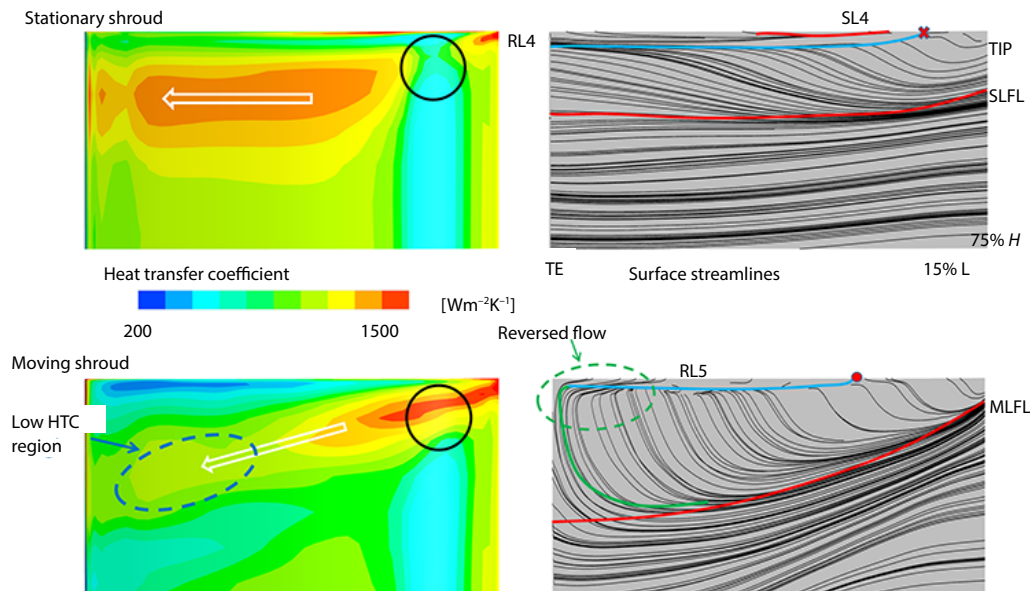


Figure 8. Heat load and surface streamlines on the upper suction surface

The angle is consistent with the movement of the leakage vortex. The HTC compared with the shroud movement case and the shroud stationary case has a large difference. The scrap-

ing vortex generated by shroud movement makes the leakage vortex near to the suction surface, so it is suppressed in the black solid line area. The flow separation creates a high HTC area.

The wall surface flow streamline further explains the flow characteristics at the suction surface and the reason of the HTC distribution. When in the stationary case, a separation-line (SL4) corresponding to the HTC, a leakage flow shock flow line (SLFL) corresponding to a high HTC, and a re-attachment line (RL4) corresponding to a low HTC are formed, respectively. When the shroud moves, a leakage flow shock streamline (MLFL) corresponding to a high HTC and a re-attachment line (RL5) corresponding to a low HTC are formed, respectively.

It is worth noting that the starting points of RL4 and RL5 are the same as the RL2 and RL3 which indicate that the shroud attachment line and the suction surface attachment line are formed by the same vortex structure.

A local backflow was formed on green dashed area in the moving case. Because the instability of the vortex core in this area caused the reverse flow of the flow velocity to form a break vortex. The leakage vortex increases the mixing and dissipation by splitting the surrounding low energy fluid which weakens the impact of the leakage flow on the suction surface wall.

#### Interaction between leakage flow and main flow

Figure 9 shows that when the shroud is stationary, the leakage flow forms a strong blockage close to the pressure surface and generates a separate flow there, which significantly makes the HTC of blade tip in this area lower.

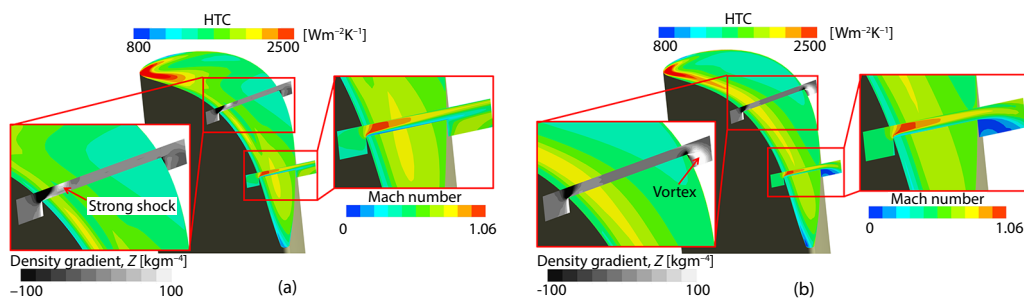


Figure 9. Contours of tip HTC and z-component of density gradient on a cut plane and Mach number on another cut plane; (a) stationary shroud and (b) moving shroud

As shroud moves, the tangential direction viscous forces caused by the end wall movement eliminate this blockage. Shroud movement has a little affected on Mach number distribution in the gap, but Mach number has increased at exit of the gap due to the effect of the suction vortex suction.

Figure 10 shows the leakage streamlines and total pressure loss (the ratio of the local total pressure  $P_{local}^*$  to the inlet total pressure  $P_{in}^*$ ) at different axial chords. It can be seen that when the shroud is moving, the leakage flow moves toward the trailing edge due to the deflection effect, while when the shroud is stationary, the leakage flow is mainly concentrated in the front

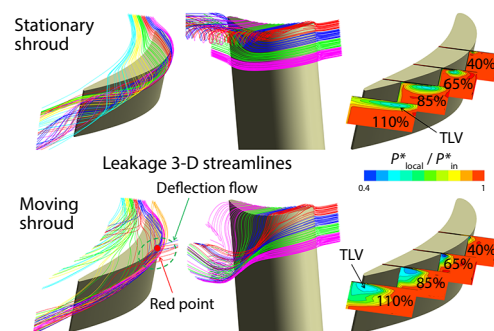


Figure 10. Leakage 3-D streamlines and total pressure loss at four axial chords

region. The flow began to converge in the green dashed area, and then developed downstream to form a leaking vortex. This area was located near the red point, further explaining the reason for the starting point of the re-attachment line (RL3, RL5) when the shroud move. The separation flow generated at the leading edge of the main stream is subjected to the leakage of the leakage vortex on the suction side, and a clear passage vortex is formed below the leakage vortex. The leakage vortex gradually moves away from the suction surface in the axial direction when the shroud is stationary, the vortex size remains unchanged in the radial direction, and the vortex size gradually increases in the circumferential direction. When the shroud moves, the leaking vortex moves downwards against the suction surface in the flow direction. At the same time, the size of the vortex core gradually increases, and the separation of the leaking vortex from the passage flow is enlarged.

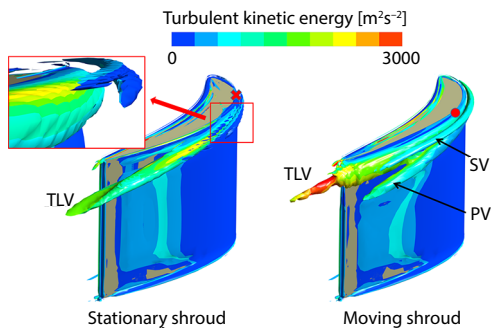


Figure 11. Turbulent kinetic energy near the tip

edge of the leaking vortex. Generally, the intensity of the turbulent kinetic energy of the leaking vortex is higher than other vortex structures.

Figure 12 shows the isentropic Mach number of the blade tip surface and the axial vorticity distribution at each section. The positive and negative values of the axial vorticity indicate the vortex rotation direction, which is in accordance with the right-hand rule. Compared with the stationary case, the movement of the shroud forms a complex vortex structure at various sections, including a clockwise leakage vortex and a trailing edge shedding vortex, a counterclockwise scraping vortex and a channel vortex.

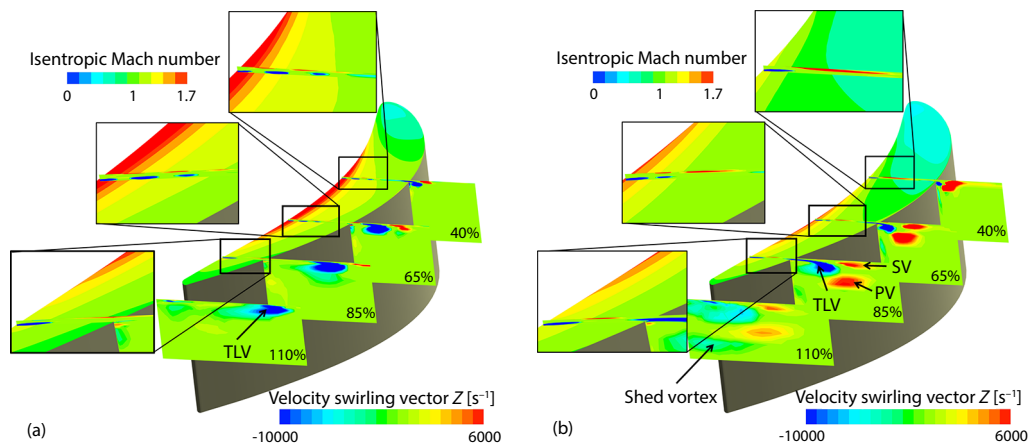


Figure 12. Contours of isentropic Mach number and Z-component of tip vortex structure at different cut planes; (a) stationary shroud and (b) moving shroud

Figure 11 shows the 3-D vortex structure and the turbulent kinetic energy distribution visualized by the  $Q$  criterion near the apex region. When the shroud is stationary, there is only one leakage vortex (TLV). When the shroud is moving, three vortex structures are formed, including leakage vortex, scraping vortex (SV), and channel vortex (PV). When the shroud is moving, the turbulent kinetic energy intensity of the vortex structure is significantly higher than that of the stationary case. The maximum turbulent kinetic energy region appears after the trailing

It is worth noting that the  $Q$ -criterion reflects the symmetry and anti-symmetry of the velocity gradient tensor, so vortex structure caused by rotation is obtained, and the axial vorticity can further reflect the vorticity caused by non-rotational motion such as shedding of the surface layer. Therefore, in combination with the results of fig. 11, it can be seen that the formation of the scraping vortex is related to the rotational shearing effect caused by the movement of the shroud and the separation flow in the near-front edge region.

The formation of the trailing edge shedding vortex is mainly related to the shedding of the wall surface attachment layer. In the blade tip, whether the shroud is moving or not, the attachment of the wall boundary-layer in the supersonic region under the action of strong shear causes the axial vorticity structure to alternate. This is closely related to the supersonic region.

Figure 13 shows streamwise velocity and temperature distribution at four different axial chords. The velocity and temperature distributions of the cross-sections are basically the same as those of the leakage vortex distribution. The flow velocity decreases and the temperature increases at the leakage vortex core. When the shroud is moving, the flow direction velocity of the 85% cross-section and the 110% cross-section area is negative which means the backflow of vortex breaking occurs. The boundary area of the vortex crushing (3-D blue area) is defined by the boundary region with a flow velocity of 0. The vortex crushing region starts at approximately 65% of the cross-section and gradually expands along the flow direction and extends to the trailing edge region.

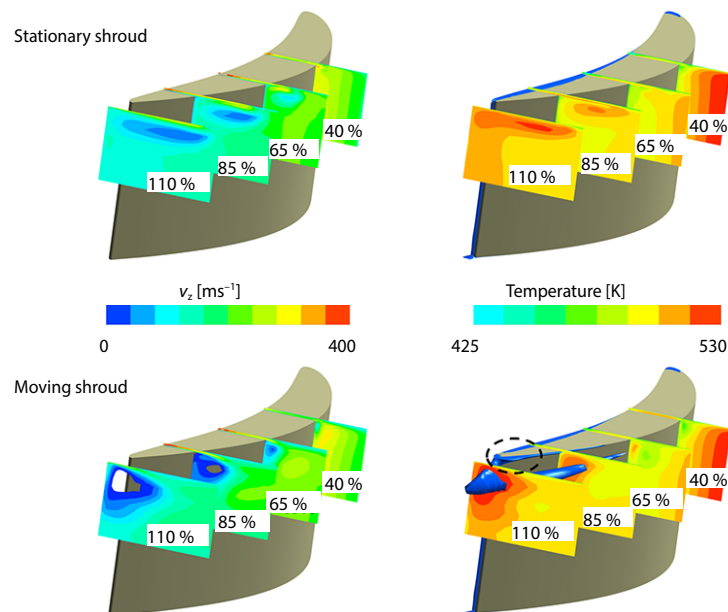


Figure 13. Streamwise velocity and temperature distribution at four axial chords

#### Overall aerothermal performance

Figure 14 shows the average HTC of different parts of blade whether the shroud is stationary and moving. The average HTC of blade tip is highest, but the change is not obvious when the shroud is moving, and the value is slightly reduced.

During the movement of the shroud, the average HTC of the shroud changed and the HTC increased significantly, increasing by 53.8%.

The average HTC of the suction surface is also relatively large. On the contrary, the movement of the shroud makes the average HTC reduced, so that average HTC of suction surface of all parts is the lowest, with a reduction of 11.9%. The previous results directly indicate that the shroud movement has a greater effect on the heat transfer characteristics near the tip of blade.

Figure 15 shows the average total pressure loss at different sections of the case when the shroud is stationary or moving. When the shroud is moving, the total pressure loss at all sections is greater than when the case is stationary. The closer the section is to the trailing edge, the greater of the total pressure loss. There are two main reasons, first reason is that the movement of the shroud increases the turbulent kinetic energy intensity at the vortex core and increases the blending loss; second reason is that when the shroud moves, the range of the vortex along the flow direction gradually expands, which enlarge the total pressure loss.

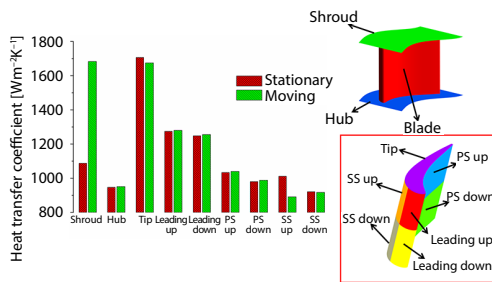


Figure 14. Average HTC at the different rotor parts

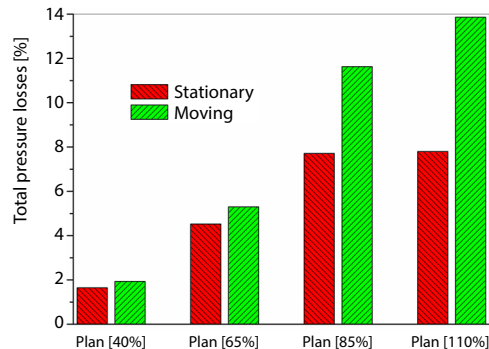


Figure 15. Average total pressure loss at different sections

## Conclusions

In this paper, a SST turbulence model based on  $\gamma$ - $\theta$  transition is used to perform a 3-D aerothermal calculation of the GE-E<sup>3</sup> first-stage blade and the following conclusions were obtained as follows.

- The deflection flow caused by the shroud movement changes the distribution of the re-attachment and SL near the blade tip which significantly changes the HTC distribution.
- The tangential viscous force generated by the end wall motion eliminates flow blocking near the pressure side of the gap and reduces the range of the transonic region in the gap. The Mach number of the gap exit increases due to the effect of the suction of the leakage vortex.
- The deflected flow caused by the shroud movement and the separated flow from the leading edge are important reasons that caused the difference in the vortex structure. The reverse pressure gradient and the radical change of the leakage vortex cause the leakage vortex to be broken.
- The movement of the shroud significantly increases the average HTC of the shroud and reduces the average HTC at the half of the suction surface. The movement has a relatively small impact on the average HTC of the blade tip, but the blade tip bears the highest heat load.

## Nomenclature

$C_p$  – static pressure coefficient, [-]  
 $H$  – blade height  
 $P$  – static pressure, [Pa]  
 $P^*$  – total pressure, [Pa]  
 $v_{in}$  – velocity, [ms<sup>-1</sup>]  
 $v_2$  – streamwise velocity

### Greek symbols

$\rho$  – density, [kgm<sup>-3</sup>]  
 $k-\omega$  – turbulence model

$\gamma-\theta$  – turbulence transition

### Acronyms

HPT – high pressure turbine, [-]  
HTC – heat transfer coefficient, [Wm<sup>-2</sup>K<sup>-1</sup>]  
TE – trailing edge

### Subscripts

in – inlet, [-]  
local – local position, [-]

## References

- [1] Bunker, R. S., Axial Turbine Blade Tips: Function, Design and Durability, *AIAA Journal of Propulsion and Power*, 22 (2006), 2, pp. 271-285
- [2] Dong, H. R., et al., Effect of Vane/Blade Relative Position on Heat Transfer Characteristics in a Stationary Turbine Blade – Part 1: Tip and Shroud, *International Journal of Thermal Sciences*, 47 (2008), 11, pp. 1544-1554
- [3] Dong, H. R., et al., Effect of Vane/Blade Relative Position on Heat Transfer Characteristics in a Stationary Turbine Blade – Part 2: Blade Surface, *International Journal of Thermal Sciences*, 47 (2008), 11, pp. 1528-1543
- [4] Yu, H. D., Theoretically and Numerically Investigation about the Novel Evaluating Standard for Convective Heat Transfer Enhancement Based on the Entransy Theory, *International Journal of Heat and Mass Transfer*, 98 (2016), 2, pp. 183-192
- [5] Vadivelu, M., Parametric Analysis and Optimization of Convective Fin with Variable Thermal Conductivity Using, *Semi-Analytical Solution*, 36 (2018), 2, pp. 677-686
- [6] Mayle, R. E., et al., Heat Transfer at the Tip of an Unshrouded Turbine Blade, *Proceedings*, 7<sup>th</sup> International Heat Transfer Conference, Munich, Germany, 1982
- [7] Metzger, D. E., et al., Cavity Heat Transfer on a Transverse Grooved Wall in a Narrow Flow Channel, *ASME Journal of Heat Transfer*, 111 (1989), 1, pp. 73-79
- [8] Srinivasan, V., et al., Effect of Endwall Motion on Blade Tip Heat Transfer, *ASME Journal of Turbomachinery*, 125 (2003), 2, pp. 267-273
- [9] Yang, J. G., et al., Numerical Investigation on Rotating Effects for an Annular Turbine Rotor Cascade, *Journal of Propulsion Technology*, 38 (2017), 10, pp. 2280-2289
- [10] Yang, D., et al., Investigation of Leakage Flow and Heat Transfer in a Gas Turbine Blade Tip with Emphasis on the Effect of Rotation, *Journal of Turbomachinery*, 132 (2010), 2, 041010
- [11] Thorpe, S. J., et al., An Investigation of the Heat Transfer and Static Pressure on the Over-tip Shroud Wall of an Axial Turbine Operating at Engine Representative Flow Conditions (I) Time-Mean Results, *International Journal of Heat Fluid-Flow*, 25 (2004), 6, pp. 933-944
- [12] Zakaria, M., et al., Computational Investigation of Heat Load and Secondary Flows Near Tip Region in a Transonic Turbine Rotor with Moving Shroud, *Applied Thermal Engineering*, 136 (2018), May, pp. 141-151
- [13] Gao, J., et al., Aerothermal Characteristics of a Transonic Tip Flow in a Turbine Cascade with Tip Clearance Variations, *Applied Thermal Engineering*, 107 (2016), Aug., pp. 271-283
- [14] Timko, L. P., Energy Efficient Engine High Pressure Turbine Component Test Performance Report, NASA Contractor Report, NASA, Washinton D.C., 168289
- [15] Bunker, R. S., Gas Turbine Cooling: Moving from Macro to Micro Cooling, *Proceedings*, ASME Turbo Expo: Turbine Technical Conference, San Antonio, Tex., USA, GT2013-94277
- [16] Celik, I. B., Procedure for Estimation and Reporting of Uncertainty Due to Discretization in CFD Applications, *ASME Journal of Fluids Engineering*, 130 (2008), 7, pp. 780011-780014
- [17] Kwak, J. S., Heat Transfer Coefficient on a Gas Turbine Blade Tip and Near Tip Regions, *AIAA Paper*, (2002), June, pp. 2002-3012
- [18] Azad, G. S., Heat Transfer and Pressure Distributions on a Gas Turbine Blade Tip, *ASME Journal of Turbomachinery*, 122 (2000), 4, pp. 717-724